Australian Journal of Basic and Applied Sciences, 9(37) Special 2015, Pages: 245-255

ISSN:1991-8178

Australian Journal of Basic and Applied Sciences

Journal home page: www.ajbasweb.com

Impact of Suction on A Stagnation–Point Flow of Copper Nanofluids Over A Vertical Porous Plate In The Presence of Magnetic Field

[1]Ashwin KumarErode Natarajan, [2]Norasikin Mat Isa, [3]Vibhu Vignesh Balachandar, [4]Kandasamy Ramasamy

[1]Master's degree student of Mechanical and Manufacturing Engineering, FKMP, UTHM, Parit raja, BatuPahat – 86400.
[2]Senior Lecturer of JabatanKejuruteraan Tenaga danTermobendalir, FKMP, UTHM, Parit raja, BatuPahat – 86400.
[3]Master's degree student of Mechanical and Manufacturing Engineering, FKMP, UTHM, Parit raja, BatuPahat – 86400.
[4]Professor of Computational Fluid Dynamics, FSSW, UTHM, Parit raja, BatuPahat – 86400.

ARTICLE INFO

Article history:
Received 10 October 2015
Accepted 30 November 2015
Available online 31 December 2015

Keywords:
Sea water/fresh water based copper nanofluid, Navier-Stokes equation, stretching/shrinking porous surface, similarity transformation, thermal radiation and heat source.

ABSTRACT

The aim of this paper is to analysethe steady stagnation-point flow and heat transfer of an incompressible nanofluids towards a shrinking/stretching surface. The governing Navier-Stokes' partial differential equations are transformed to a set of nonlinear ordinary differential equations by means of a similarity transformation. A comparison analyses on sea water/fresh water based copper nanofluids is presented to investigate the effect of suction under the influence of pertinent parameters such as the magnetic parameter, Grashof number, Eckert number, thermal radiation and heat generation are discussed over a vertical porous surface. The temperature and velocity distributions of nanofluids at the porous surface illustrates that Cu-sea water nanofluid has high heat transfer than the Cu-fresh water nanofluids have quite similar characteristics for all stream conditions. Sea water can be effectively used as a basefluid to replace fresh water. Comparisons with published results is presented.

ToCite ThisArticle: Ashwin Kumar Erode Natarajan, Norasikin Mat Isa, VibhuVigneshBalachandar, KandasamyRamasamy.,Impact of suction on a stagnation–point flow of copper nanofluids over a vertical porous plate in the presence of magnetic field. ***Aust. J. Basic & Appl. Sci.,*** *9(37): 245-255, 2015*

INTRODUCTION

Necessity has come in industries to develop heat transfer fluids having high heat transfer efficiencyto suit the current day power plants, electronics, and transportation in which heat transfer plays essential role. Conventional heat transfer fluids have very low thermal conductivity and has very less heat transfer efficiency.Choi (1995), introduced a new approach by using particles in nano-meter (10^{-9}) scale dispersed in a conventional fluids, known as nanofluid has been studied extensively in recent years. Eastman et al. (2001)studied copper nanofluids taking ethylene glycolas base fluid. The mean diameter of copper nanoparticles are <10nm. The results showed that there was a 40% rise in thermal conductivity, when 0.3vol% of copper nanoparticles immersed in the base fluid.Oztop and Abu-Nada (2008) presented similar results, where an increase in heat transfers was observed by the addition of nanoparticles.Mahapatra and Gupta (2001) observed the heat transfer in stagnation-point flow towards a stretching plate. The governing system of PDE was converted to ODE by using similarity transformations, then evaluated using the Keller-box method. The study was to understand the effects of the governing parameters, namely the suction/injection parameter, Prandtl number on the velocity and temperature profiles. MHD stagnation-point flow and boundary layer flow is studied by Mahapatra and Gupta (2002) and Ishak and Nazar (2008) over a stretching surface. According to their results, it is clear that when stretching velocity is lower than that of free stream velocity, there is an increase in velocity at one point with an increase in magnetic field.

Owing to the need of replacement of fresh water and other conventional heat transfer fluids, researches are carried all over the world to use sea water as coolant. Cooling of condensers using sea water in buildings situated near sea. Andersen (2004), investigated that by using sea water, energy used for generation of cooling can be saved up to up to 30%. Proper understanding of the behaviour of sea water as coolant will be of great benefit in general. The physical properties of seawater include both thermodynamic properties' like density and freezing point, as well as 'transport properties' like the electrical conductivity and viscosity. Pawlowicz(2013) stated that density is usually calculated using a mathematical function of temperature, salinity, and pressure, sometimes called

Corresponding Author: Ashwin Kumar Erode Natarajan, Master's degree student of Mechanical and Manufacturing Engineering, FKMP, UTHM, Parit Raja, BatuPahat – 86400.
Tel: +6017-7676960; Email: ashwinkumaren@gmail.com

an equation of state. Sharqawy(2010) calculated thermo-physical properties by changing temperature and salinity.

The objective of the present work is to study the stagnation-point flow and heat transfer characteristic of copper nanofluids of Pal et al. (2014). In this paper, we investigate the behaviour of velocity and temperature profiles of sea water/fresh water based copper nanofluids in the presence of magnetic field, thermal radiation, heat source, Grashof number and Eckert number in the presence of injection on the stretching/shrinking wall.

Nomenclature:

Symbol	Quantity	units
B_0	Magnetic field strength	N/Am
Cu	Copper	
C_p	Specify heat of solid	m^2/s^2K
Ec	Eckert number	Nil
$f'(\eta)$	Velocity	Nil
Gr	Grashof number	Nil
G	Gravitational force	m/s^2
K_1	Permeability of the porous medium	m^2
K^*	Mean spectral absorption coefficient	1/m
M	Magnetic field strength parameter	$Nm/\Omega A^2 s^1$
MHD	Magnetohydrodynamics	N
N	Thermal radiation parameter	s^3/m^2
ODE	Ordinary differential equations	Nil
PDE	Partial differential equations	Nil
Pr	Prandtl number	Nil
Q_o	Heat generation/absorption coefficient	$kg/m^1s^3K^1$
Re	Reynolds number	Nil
S	Injection velocity parameter	Nil
T	Temperature	K
u, v	Velocity components in x,*y*-directions respectively	m/s
u_w	Stretching or shrinking surface velocity	m/s
U	Free stream velocity of the nanofluid	m/s
2-D	Two dimensional	Nil
Greek letters		
α	T hermal diffusivity	m^2/s
β	Thermal expansion coefficient	1/K
γ	Buoyancy parameter	Nil
H	Similarity variable	Nil
$\theta(\eta)$	temperature of the fluid	Nil
θ_w	Wall temperature excess ratio parameter	Nil
$\theta'(\eta)$	heat transfer rate	Nil
κ	Thermal conductivity	kgm/s^3K
Λ	Heat sink/source parameter	Nil
μ	Dynamic viscosity	kg/ms
ρ	Density	kg/m^3
ρC_p	Heat capacitance	J/m^3K
σ	Electrical conductivity	$1/\Omega m$
σ^*	Stefan–Boltzmann constant	kg/m^2K^4
ϕ	Nanoparticles volume fraction	vol%
Ψ	Stream function	m^2/s
Subscripts		
nf	Nanofluid	
f	Fluid	
s	Solid	

Mathematical Analysis:

The flow model for achieving our objectives is shown in fig. 1. In this study, the nanofluid flow is selected to be a 2-D stagnation-point flow, over a permeable plate. The plate is subjected to shrinking and stretching; for stretching plate the linear velocity over a porous plate is $u_w = cx$ and the velocity over a porous plate becomes negative for shrinking plate that is $u_w = -cx$. The flow is time independent and laminar flow. $U(x) = ax$is defined as the free stream flow. Magnetic field strength (B_0) which is present in positive x-axis, influences the nanofluid flow. Nanoparticles and base fluids are assumed to be in thermal equilibrium and no slip occurs between them. The acceleration due to gravity is denoted by g. The thermo-physical properties of base fluid and nanoparticle is given in Table 1. Prandtl number of

fresh water is taken as 6.2 at 20℃.Sea water with Pr =7.155 at 20℃, salinity = 35 °/oo.

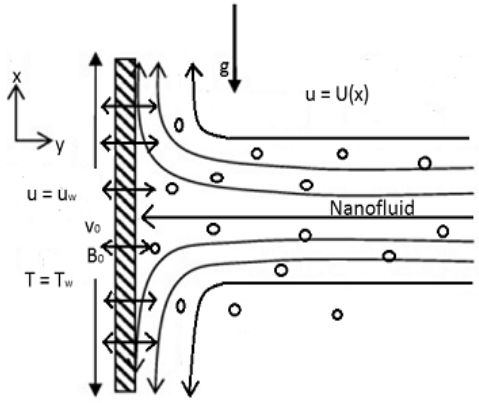

Fig. 3.1: Stagnation-point flow model over a vertical permeable plate

Table 3.1: Thermo-physical properties of fluid and copper nanoparticle. [Oztop and Abu-Nada (2008),Sharqawy(2010)]

Physical properties	Fresh water at 20℃	Sea water at 20℃ (Salinity=35g/kg)	Cu
C_p	4179	4000	385
ρ	997.1	1025	8933
κ	0.613	0.6015	401

With above assumptions, the boundary layer equations are as follows:

$$\frac{\partial u}{\partial x}+\frac{\partial v}{\partial y}=0 \tag{1}$$

$$u\frac{\partial u}{\partial x}+v\frac{\partial v}{\partial y}=U(x)\frac{dU(x)}{dx}+\frac{\mu_{nf}}{\rho_{nf}}\frac{\partial^2 u}{\partial y^2}+\frac{\mu_{nf}}{\rho_{nf}K}(U(x)-u) \tag{2}$$

$$\left.\begin{aligned}u\frac{\partial T}{\partial x}+v\frac{\partial T}{\partial y}=\alpha_{nf}\frac{d^2T}{dy^2}+\frac{Q_0}{(\rho C_p)_{nf}}(T-T_\infty)-\\ \frac{1}{(\rho c_p)_{nf}}\frac{\partial q_r}{\partial y}+\frac{\mu_{nf}}{(\rho c_p)_{nf}}\left(\frac{\partial u}{\partial y}\right)^2\end{aligned}\right\} \tag{3}$$

Subjected to the boundary conditions (for shrinking or stretching plate)

$$\left.\begin{aligned}v=v_0, u=u_w(x)=\pm cx, T=T_w \text{ at } y=0;\\ T\to T_\infty, u\to U(x)=ax, C\to C_\infty \text{ as } y\to\infty\end{aligned}\right\} \tag{4}$$

For calculating density, thermal conductivity, dynamic viscosity, thermal diffusivity and heat capacitance of nanofluids the below mentioned equations are used.

$$\rho_{nf}=(1-\phi)\rho_f+\phi\rho_s \tag{5}$$

$$\kappa_{nf}=\kappa_f\left[\frac{\kappa_s+2\kappa_f-2\phi(\kappa_s-\kappa_f)}{\kappa_s+2\kappa_f+2\phi(\kappa_s-\kappa_f)}\right] \tag{6}$$

$$\mu_{nf}=\frac{\mu_f}{(1-\phi)^{2.5}} \tag{7}$$

$$(\rho C_p)_{nf}=(1-\phi)(\rho C_p)_f+\phi(\rho C_p)_s \tag{8}$$

$$\alpha_{nf}=\frac{\kappa_{nf}}{(\rho c_p)_{nf}} \tag{9}$$

Eq. (1) to Eq. (3) is transformed using similarity functions, the stream function are

$$\left.\begin{aligned}\psi=\sqrt{c\cdot\nu_f}\cdot f(\eta)\cdot x,\quad \eta=\sqrt{\frac{c}{\nu_f}}\cdot y,\\ (T_W-T_\infty)\,\theta(\eta)=T-T_\infty\end{aligned}\right\} \tag{10}$$

$$\theta_w=\frac{T_W}{T_\infty} \tag{11}$$

Defining the stream function ψ that is, (u) = ψ_y, (v) = -ψ_x, which satisfies the Eq. (1) and Eq. (5) to Eq. (9) are substituted into Eq. (2), Eq. (3) and Eq. (4), we get following non-linear ODE:

$$\left.\begin{aligned} &f''' + ((1-\phi)^{2.5}M + K)\left(\frac{a}{c} - f'\right) + (1-\phi)^{2.5} \\ &\left(1-\phi+\phi\frac{\rho_s}{\rho_f}\right)\left(\frac{a^2}{c^2} + ff'' - f'^2 + \gamma\theta\right) = 0 \end{aligned}\right\} \quad (12)$$

$$\left.\begin{aligned} &\theta'' + \frac{Pr}{\left(\frac{\kappa_{nf}}{\kappa_f} + N(1+(\theta_w-1)\theta)^3\right)} \cdot \\ &\left[\begin{aligned} &\frac{3N}{Pr}.(\theta_w-1)(1+(\theta_w-1)\theta)^2\theta'^2 + \\ &\left(1-\phi+\phi\frac{(\rho c_p)_s}{(\rho c_p)_f}\right)(F\theta' - 2F'\theta) + \lambda\theta \\ &+\frac{Ec}{(1-\phi)^{2.5}}\theta' \end{aligned}\right] = 0 \end{aligned}\right\} \quad (13)$$

Boundary conditions for stretching and shrinking plate:

$$\left.\begin{aligned} &f = S,\ f' = 1, \theta = 1 \text{ at } \eta = 0 \text{ (stretching)} \\ &f = S,\ f' = -1, \theta = 1 \text{ at } \eta = 0 \text{ (shrinking)} \\ &f' \to \frac{a}{c}, \theta \to 0,\ \eta \to \infty \end{aligned}\right\} \text{ y=0} \quad (14)$$

$Pr = \frac{v}{\alpha}$ is the Prandtl number, $Ec = \frac{{u_w}^2}{c_p \Delta T}$ is the Eckerts number, $Gr = \frac{g\beta(T_w - T_\infty)x^3}{v^2}$ is the Grashof number, $\gamma = \frac{Gr}{Re^2}$ is the Buoyancy parameter, $S = -\frac{v_w}{\sqrt{cv_f}}$ is the injection parameter, $\lambda = \frac{Q_0 v_f}{c\kappa_{nf}}$ is the heat source/sink, $K = \frac{v_f}{cK_1}$ is the porous parameter, $N = \frac{16\sigma^* T_f^3}{3k_f k^*}$ is the thermal radiation parameter and $M = \frac{\sigma B_0^2}{\rho_f c}$ is the magnetic parameter.

For validating the results obtained from MAPLE 18 software, the values for the parameters as given in previously presented journals by Mahaputra and Gupta (2002), Hamad and Pop (2010), Pal et al. (2014)are given in MAPLE 18 software to obtain heat transfer rate values and velocity profiles. From Table 3.2, the dimensionless heat transfer rates obtained from MAPLE 18 software is in agreement with previously published journals by Mahaputra and Gupta (2003), Hamad and Pop (2010). From Figure3.2 and Figure 3.3, the velocity profiles obtained in MAPLE 18 software is in perfect correlation with that of results of Pal et al. (2014).

Table 3.2: Comparison of –θ'(0) obtained from MAPLE software with published works for stretching plate

Pr	a/c	Mahapatra and Gupta (2002)	Hamad and Pop (2010)	Present results
1	0.1	0.625	0.6216	0.62537
	1	0.796	0.8001	0.79967
	2	1.124	1.1221	1.12375
1.5	0.1	0.797	0.7952	0.79500
	1	0.974	0.7952	0.79503
	2	1.341	1.3419	1.34095

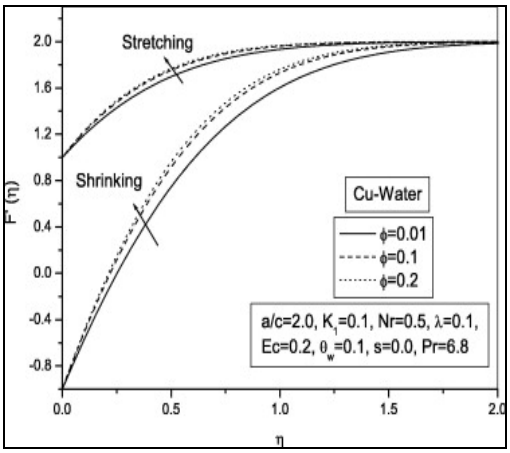

Fig. 3.2: Nanoparticle volume fraction effect on copper nanofluid Pal et al. (2014)

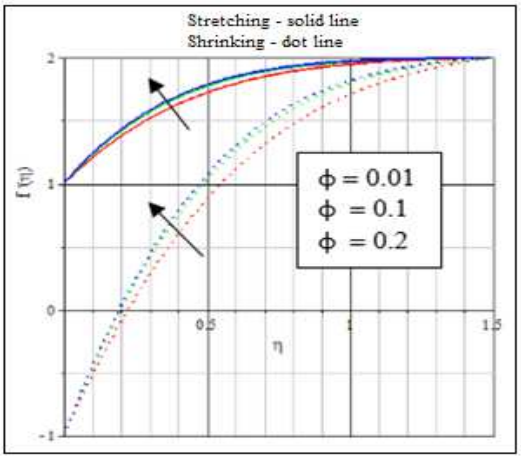

Fig. 3.3: Nanoparticle volume fraction effect on copper nanofluid (MAPLE 18 software)

RESULT AND DISCUSSION

The set of equations (12) and (13) is highly nonlinear. Hence coupled and cannot be solved analytically and numerical solutions subject to the boundary conditions (14) are obtained using the very robust computer algebra software Maple 18. This software uses a fourth-fifth order Runge–Kutta–Fehlberg method as default to solve boundary value problems numerically using the dsolve command. The transformed system of coupled nonlinear ordinary differential Equations (12) and (13) including boundary conditions (14) depend on the various parameters. Table 4.1 shows the stream conditions for studying the behaviour of nanofluids. The parameter to be studied is given three different values, all other parameters which are under consideration are fixed.

Table 4.1: Stream conditions (From Figure 4.1 to Figure 4.20)

Figures	Parameters	Fixed parameters
4.1 - 4.4	Magnetic field strength (M) = 1, 3, 5	Pr = 6.2, a/c = 2, ϕ= 0.2,Gr = 3, K = 0.1, θ_w = 0.5, S = 1/-1,M = 1, λ = 0.1, N = 1, Ec = 0.2
4.5 - 4.8	Heat source λ = 1, 4, 7	
4.9 - 4.12	Thermal radiation (N) = 1, 5, 10	
4.13 - 4.16	Grashof number (Gr) = 1, 3, 5	
4.17 – 4.20	Eckert number (Ec) = 0.1, 0.2, 0.4	

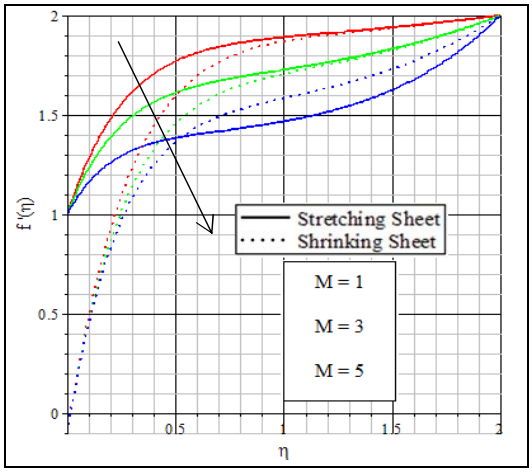

Fig. 4.1: Magnetic effects on velocity profiles over Cu-sea water in the presence of suction

Figure 4.1 to Figure 4.2 present the velocity profiles for Cu-sea water and Cu-fresh water for suction velocities for different values of M. Suction causes the flow to decelerate the fluid flow. Hence in addition to the effects of M in decelerating the flow by opposing force known as Lorentz force, the suction causes more deceleration to the nanofluid flow. From Figure 4.43 to Figure 4.46, Cu-sea water nanofluid has less velocity than the Cu-freshwater nanofluid. The order of magnitude in variation among the velocity profiles both the nanofluids is very less.

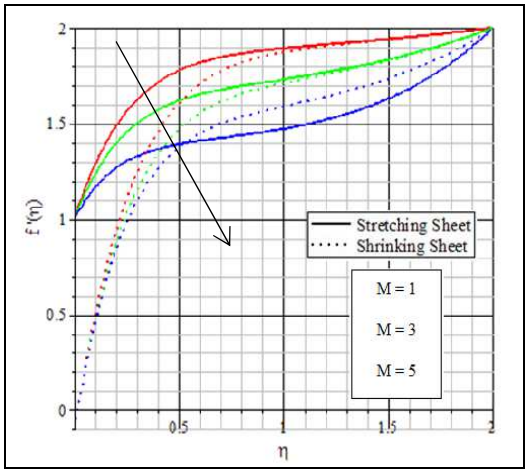

Fig. 4.2: Magnetic effects on velocity profiles over Cu-fresh water in the presence of suction

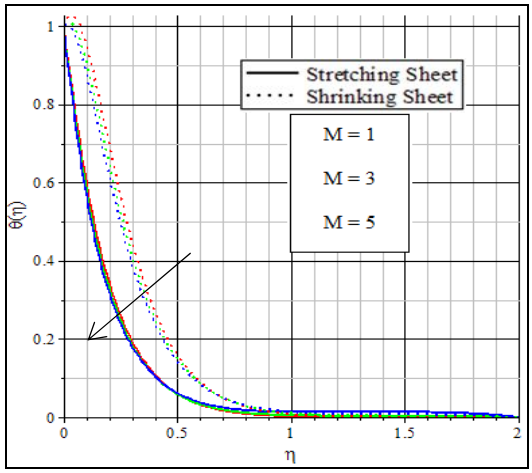

Fig. 4.3: Magnetic effects on temperature profiles over Cu-sea water in the presence of suction

From Figure 4.3 to Figure 4.4, temperatures profiles for Cu-sea water and Cu-fresh water in the presence of suction for different values of M is analyzed. The temperature distribution is higher in case of shrinking than stretching surfaces. In the presence of suction, it is also observed that the thermal boundary layer thickness of shrinking surface is significantly stronger than that of stretching surface. Figure 4.3 and Figure 4.4, in the presence of suction, it is observed that the temperature of Cu-sea water and Cu-fresh water decreases for both stretching and shrinking surface with increase of M. The temperature profiles in case of suction, is effective only when the nanofluid flow is closer to boundary layer. Beyond η=1, dimensionless temperature θ(η) of both Cu-sea water and Cu-fresh water nanofluids is less than 0.1 for both shrinking and stretching surfaces and slowly tends to zero at η=2. Based on Table 3.1, it is clear that the fluid temperature distribution is reduced by the density of Cu-sea water compared to that of Cu-water and confirms the fact that the application of M to an electrically conducting fluid produces a dragline force which causes deceleration in the temperature.

The effect of heat source (λ) on velocity profiles in the presence of suction over Cu-sea water and Cu-fresh water nanofluids in shrinking and stretching surfaces. Figure 4.5, in case of suction, velocity profiles of Cu-sea water over stretching surface shows an increase in velocity profiles for increase in λ but velocity profiles in shrinking surfaces decrease for increase in λ. Figure 4.6, the velocity gradients of nanofluids over stretching surfaces becomes less beyond η = 0.6. For high values of λ, in shrinking surfaces the velocity profiles goes beyond $f'(\eta) = 2$ but when the flow is nearer to momentum boundary layer, the velocity gradient increases, as the velocity profile becomes $f'(\eta)=0$ at η = 0.02.

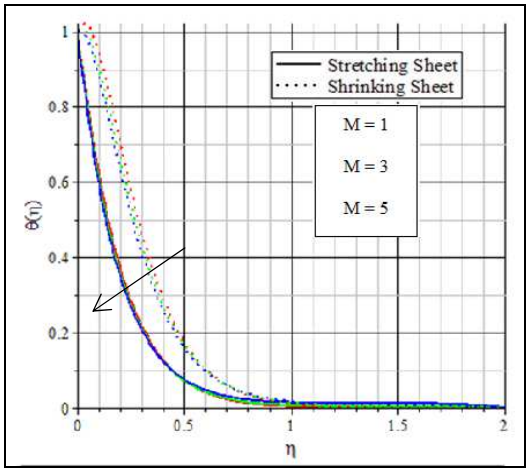

Fig. 4.4: Magnetic effects on temperature profiles over Cu-fresh water in the presence of suction

Figure 4.7 to Figure 4.8, the temperature profiles for different values of λ, is analyzed in the presence of suction. Figure 4.7, in the presence of suction, stretching surfaces increases for increase in λ. In case of shrinking surfaces, temperature increases for lower values of λ but for higher values of λ, temperature shows a sudden drop in temperature magnitude $\theta(\eta)$< -1.3. Figure 4.8, temperature profiles of both shrinking and stretching increases with increase in heat source effect on boundary layer. The temperature forms peak for higher values of λ and the temperature profile for λ = 7 in shrinking surface reaches $\theta(\eta)$ =2.4. Figure 4.7 and Figure 4.8, the temperature profiles in the presence of suction is quite effective when the flow is close to the boundary layer and tends to zero at η = 1.3 for Cu-sea water and at η = 1.5 for Cu-fresh water nanofluid.

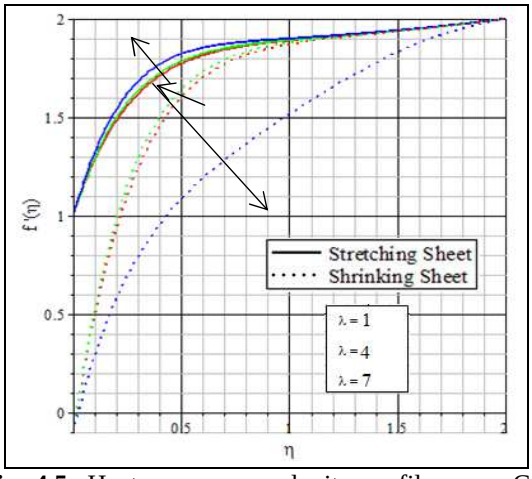

Fig. 4.5: Heat source on velocity profiles over Cu-sea water in the presence of suction

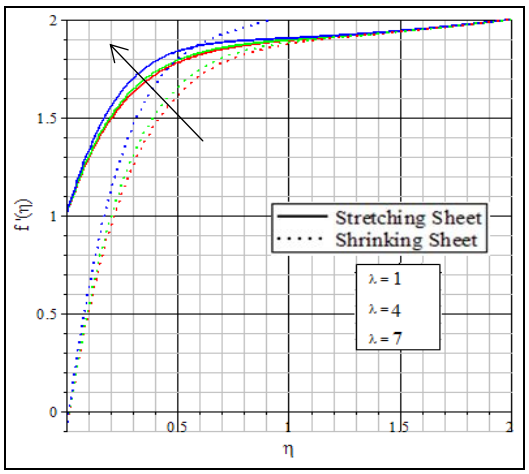

Fig. 4.6: Heat source on velocity profiles over Cu-fresh water in the presence of suction

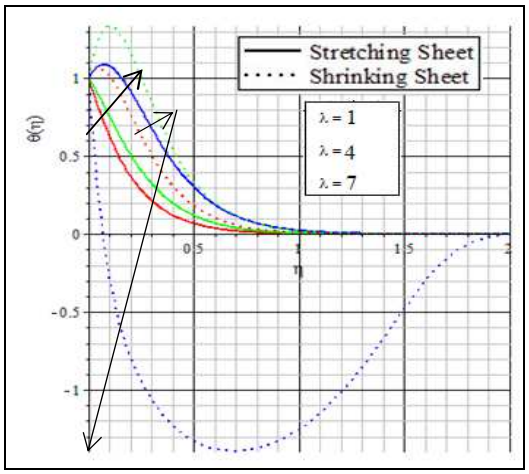

Fig. 4.7: Heat source on temperature profiles over Cu-sea water in the presence of suction

Figure 4.9 to Figure 4.10, depicts the influence of thermal radiation (N) on velocity profiles on Cu-sea water and Cu-fresh water nanofluids in the presence of suction. Velocity profiles show small deviation for increase in N in the presence of suction. Velocity profiles of Cu-sea water and Cu-fresh water is just the same in the presence of suction.

The temperature profiles of Cu-sea water and Cu-fresh water nanofluids for different values of N in the presence of suction velocity on the surfaces is shown from Figure 4.11 to Figure 4.12. The temperature profiles of stretching and shrinking surfaces decrease as the flow is near the thermal boundary layer and increase when they move out of the influence of boundary layer. The temperature profiles of stretching surfaces in the presence of suction shows only a narrow changes in magnitude. Temperature profiles tends to zero at η = 1.9 in the presence of suction. Cu-sea water and Cu-fresh water nanofluids show similar behavior in case of suction

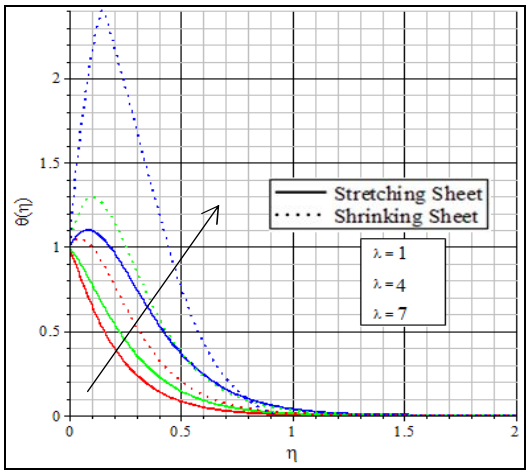

Fig. 4.8: Heat source on temperature profiles over Cu-fresh water in the presence of suction

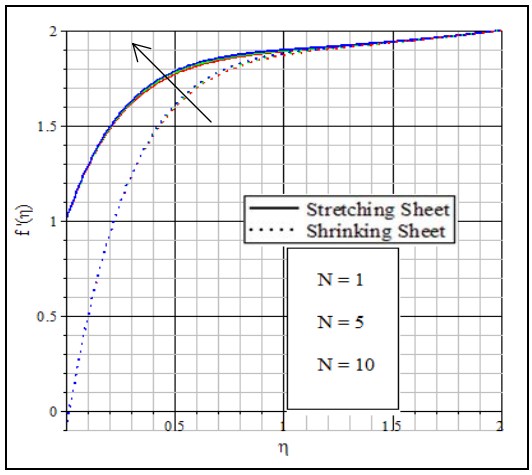

Fig. 4.9: Thermal radiation on velocity profiles over Cu-sea water in the presence of suction

Figure 4.13 to Figure 4.14 present the velocity of Cu-fresh water and Cu-sea water in the presence of suction and injection under the effects of Grashof number (Gr). Gra dimensionless number in fluiddynamics and heat transfer. Velocity profiles in shrinking surfaces is lower than the

velocity in stretching surfaces in suction. Meaning that the nanofluid flow over shrinking surfaces are retarded more than nanofluid flow in stretching. The effects of Gr in case of suction is high only near the momentum boundary layer. Velocity profiles are increasing for increasing Gr in both the cases. Very mild difference in velocity distribution is found between Cu-sea water and Cu-fresh water in the presence of suction.

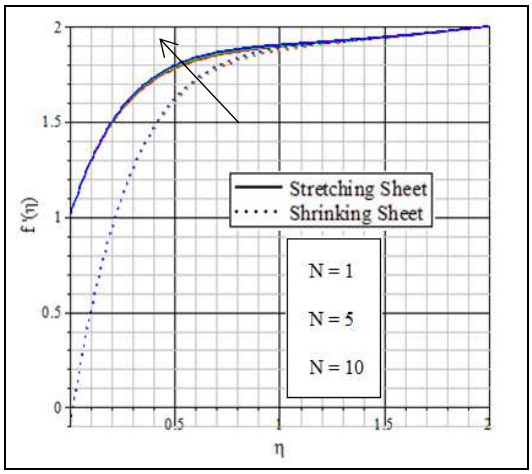

Fig. 4. 10: Thermal radiation on velocity profiles over Cu-fresh water in the presence of suction

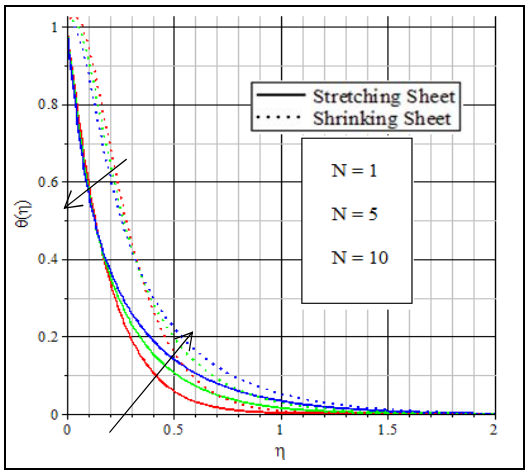

Fig. 4.11: Thermal radiation on temperature profiles over Cu-sea water in the presence of suction

Figure 4.15 to Figure 4.16, presents the Cu-sea water and Cu-fresh water nanofluids' behavior of temperature for various values of Gr. In stretching surfaces, in the temperature profiles are similar for changes in Grashof number, in case of suction. In case of stretching surfaces when the flow influenced by suction velocity the temperature profiles decreases for increasing Gr value. In Figure 4.15 and Figure 4.16, the temperature profiles of both stretching surface and shrinking surfaces tends to η = 1 and η = 1.1 respectively.

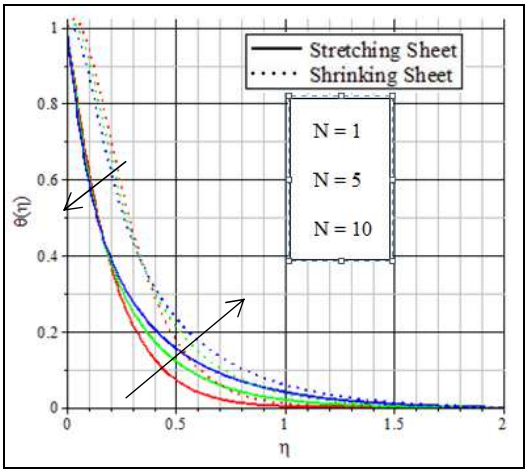

Fig. 4.12: Thermal radiation on temperature profiles over Cu-fresh water in the presence of suction

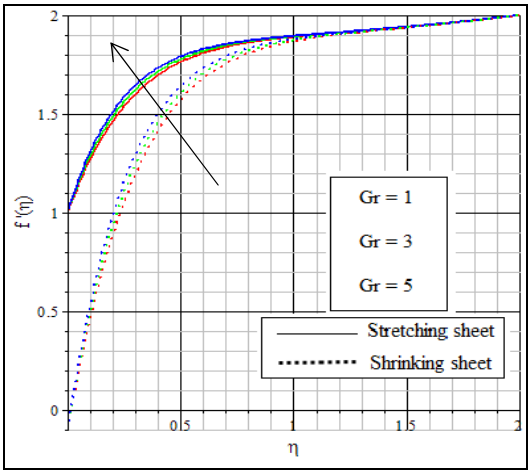

Fig. 4.13: Grashof number on velocity profiles over Cu-sea water in the presence of suction

Figure 4.17 to Figure 4.18 shows the velocity distribution over Cu-sea water and Cu-fresh water for Eckert number (Ec) in the presence of suction. In Figure 4.17 to Figure 4.18, stretching surfaces show no difference in magnitude of velocity profiles, as there is no significant changes in the presence of suction. In the presence of suction, when the nanofluid flow is over shrinking surfaces velocity profiles at η = 0.5 are above $\theta(\eta)$=1.5. For different values of Ec, Cu-seawater and Cu-fresh water nanofluids over shrinking surfaces show similar velocity profiles in the presence of suction.

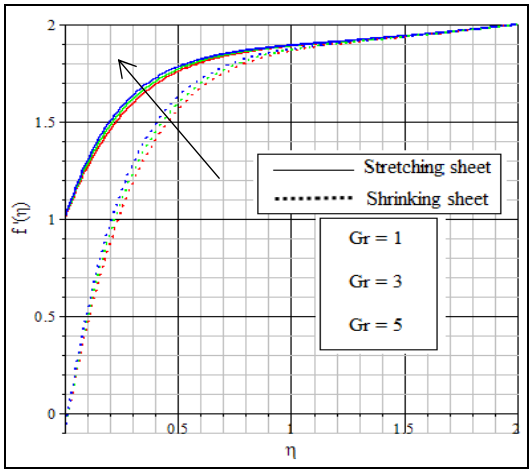

Fig. 4.14: Grashof number on velocity profiles over Cu-fresh water in the presence of suction

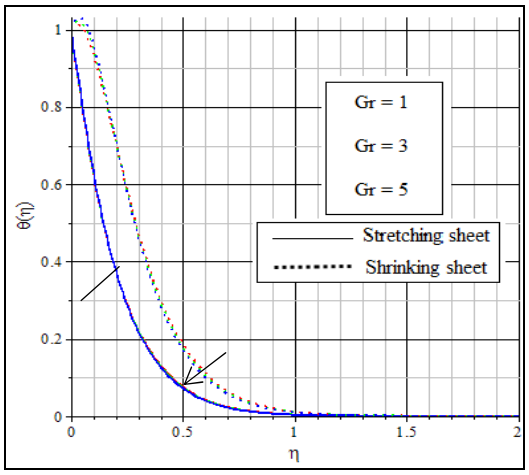

Fig. 4.15: Grashof number on temperature profiles over Cu-sea water in the presence of suction

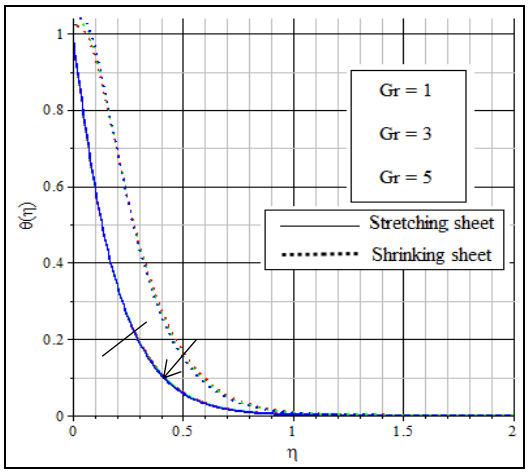

Fig. 4.16: Grashof number on temperature profiles over Cu-fresh water in the presence of suction

From Figure 4.19 to Figure 4.20, shows the influence of Eckert number (Ec) on temperature profiles of Cu-sea water and Cu-fresh water nanofluids. Eckert number is a parameter of viscous dissipation. Temperature profiles in shrinking surface shows peak formation but quite opposite results is obtained in the presence of stretching surface as there is no peak formation. The explanation for such behavior is that, when fluid is sheared there is a frictional energy loss and this energy loss is known as viscous dissipation. The energy loss is converted into heat, which increases the internal energy of the fluid that corresponds to the rise in temperature. Temperture profiles from Cu-sea water has good results than the Cu-fresh water nanofluid. The explanation for such behavior is that, specific capacity at constant presure (C_p) is high for fresh water compared to sea water as shown in Table 3.1

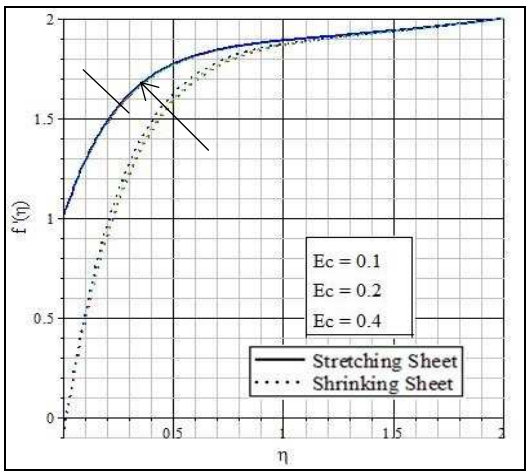

Fig. 4.17: Eckert number on velocity profiles over Cu-sea water in the presence of suction

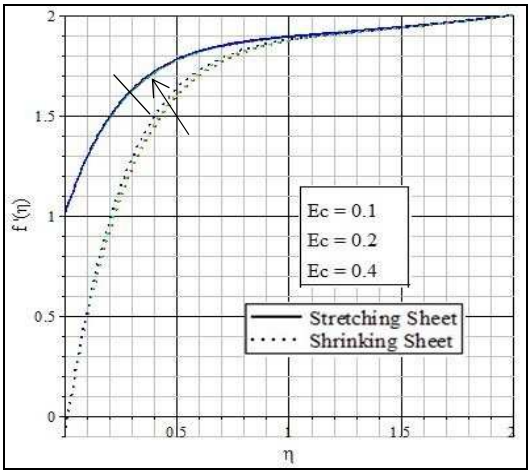

Fig. 4.18: Eckert number on velocity profiles over Cu-fresh water in the presence of suction

Higher the value of specific heat capacity(C_p) lesser the effect of Eckert number. Thus, Eckert

number has more effect on Cu-sea water nanofluid and tends to increase the internal energy causing slight rise in temperature which is evident from Figure 4.19 to Figure 4.20. The effect of Eckert number in the presence of suction is high when the nanofluid is very close to thermal boundary layer and tends to zero at $\eta = 1$ (stretching surface) and at $\eta = 1.1$ (shrinking surface).

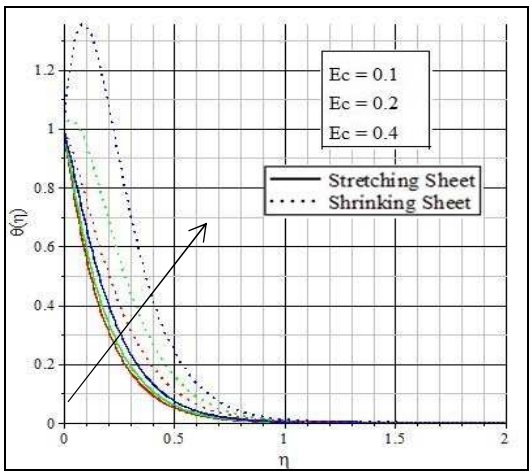

Fig. 4.19: Eckert number on temperature profiles over Cu-sea water in the presence of suction

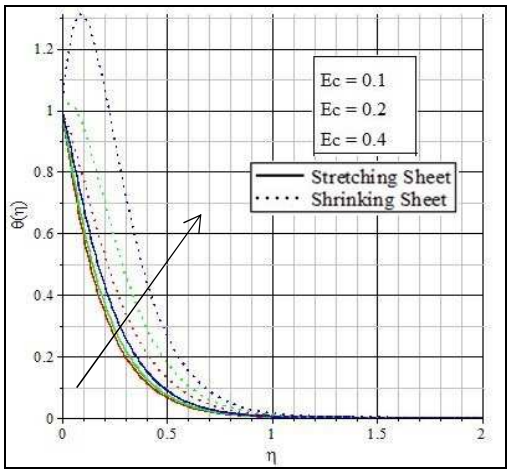

Fig. 4.20: Eckert number on temperature profiles over Cu-fresh water in the presence of suction

Conclusion:

The main objective of this research is to find out the heat transfer characteristics of the different nanofluids in stagnation-point flow and thermal conductivity enhancement of nanofluids for various parameters such as magnetic field, Thermal radiation, heat source, Eckert number, Grashof number in the presence of suction. Even though researches are carried all over the world to use sea water for cooling purposes, there is no research on nanofluids, taking sea water as base fluids. The nanofluids using fresh water and sea water as base fluid are taken into consideration and found that heat transfer efficiency is high in case of sea water based nanofluids. This data are very useful in the consideration of manufacturing sea water based nanofluids for cooling purposes.

Though there are similar work, but in the present research on heat transfer behavior of fresh water based nanofluids is compared with sea water based nanofluids in stagnation-point flow over porous surface and their performance is studied. The effect of suction factor is studied exclusively. From this study we conclude that, the sea water based nanofluid performance is efficient in stagnation-point flow over porous surfaces and high heat transfer characteristic is obtained in sea water based nanofluid and hence the fresh water based nanofluids can be effectively replaced by sea water based nanofluids in applications which is using stagnation-point flow over stretching or shrinking porous surfaces.

ACKNOWLEDGEMENT

The work was partly supported by UniversitiTun HusseinOnn Malaysia, Johor, Malaysia, under the Short Term Grant Scheme Vot.no. 1289.

REFERENCES

Andersen, D.V.B., 2004. Sea water cooling, Danish board of district heating, 1.

Choi, S., 1995. Enhancing thermal conductivity of fluids with nanoparticle, development and applications of non-Newtonian flow, Fluids Engineering Division, 231: 99-105.

Eastman, J.A., S.U.S. Choi, S. Li, W. Yu, L.J. Thomson, 2001. Anomalously increased effective thermal conductivities of ethylene glycol based nanofluids containing copper nanoparticles, Appl. Phys. Lett., 78-718-720.

Hamad, M.A.A. and I. Pop, 2010. Scaling transformations for boundary layer flow near the stagnation-point on a heated permeable stretching surface in a porous medium saturated with a nanofluid and heat generation/absorption effects, Trans. Porous Medium, 87:25-39.

Ishak, A. and R. Nazar, 2008. Uniform suction/blowing effect on flow and heat transfer due to a stretching cylinder, Appl. Math Model., 32(10): 2059-2066.

Mahapatra, T.R. and A.S. Gupta, 2001. Magnetohydrodynamics stagnation-point flow towards a stretching surface, ActaMechanica, 152(1-4): 191-196.

Mahapatra, T.R. and A.S. Gupta, 2002. Heat transfer in stagnation-point flow towards a stretching sheet, Heat Mass Trans., 38: 517-521.

Oztop, H.F. and E. Abu-Nada, 2008. Numerical study of natural convection in partially heated

rectangular enclosure filled with nanofluids, Int. J. Heat Fluid Flow, 29(5): 1326-1336.

Pal, D., G. Mandal and K. Vajravelu, 2014. Flow and heat transfer of nanofluids at a stagnation point flow over a stretching/shrinking surface in a porous medium with thermal radiation, Appl. Math Comp, 238: 208-224.

Pawlowicz, R., 2013. Key physical variables in the ocean: temperature, salinity, and density, Nature Education Knowledge, 4(4): 13.

Sharqawy, M.H., J.H.V. Lienhard and S.M. Zubair, 2010. Thermophysical Properties of Seawater: A Review of Existing Correlations and Data, Desalination and Water Treatment, 16: 354-380.